The Journal of Immunology

B7h Triggering Inhibits the Migration of Tumor Cell Lines

Chiara Dianzani, Rosalba Minelli, Casimiro Luca Gigliotti, Sergio Occhipinti, Mirella Giovarelli, Laura Conti, Elena Boggio, Yogesh Shivakumar, Gianluca Baldanzi, Valeria Malacarne, Elisabetta Orilieri, Giuseppe Cappellano, Roberto Fantozzi, Daniele Sblattero, Junji Yagi, Josè Maria Rojo, Annalisa Chiocchetti and Umberto Dianzani

J Immunol 2014; 192:4921-4931; Prepublished online 11 April 2014;
doi: 10.4049/jimmunol.1300587
http://www.jimmunol.org/content/192/10/4921

The Journal of Immunology is published twice each month by
The American Association of Immunologists, Inc.,
9650 Rockville Pike, Bethesda, MD 20814-3994.

Print ISSN: 0022-1767 Online ISSN: 1550-6606.

B7h Triggering Inhibits the Migration of Tumor Cell Lines

Chiara Dianzani,* Rosalba Minelli,* Casimiro Luca Gigliotti,† Sergio Occhipinti,‡ Mirella Giovarelli,‡ Laura Conti,‡ Elena Boggio,† Yogesh Shivakumar,† Gianluca Baldanzi,§ Valeria Malacarne,§ Elisabetta Orilieri,† Giuseppe Cappellano,† Roberto Fantozzi,* Daniele Sblattero,† Junji Yagi,¶ Josè Maria Rojo,‖ Annalisa Chiocchetti,† and Umberto Dianzani†

Vascular endothelial cells (ECs) and several cancer cells express B7h, which is the ligand of the ICOS T cell costimulatory molecule. We have previously shown that B7h triggering via a soluble form of ICOS (ICOS-Fc) inhibits the adhesion of polymorphonuclear and tumor cell lines to HUVECs; thus, we suggested that ICOS-Fc may act as an anti-inflammatory and antitumor agent. Because cancer cell migration and angiogenesis are crucial for metastasis dissemination, the aim of this work was to evaluate the effect of ICOS-Fc on the migration of cancer cells and ECs. ICOS-Fc specifically inhibited the migration of HUVECs, human dermal lymphatic ECs, and the HT29, HCT116, PC-3, HepG2, JR8, and M14 tumor cell lines expressing high levels of B7h, whereas it was ineffective in the RPMI7932, PCF-2, LM, and BHT-101 cell lines expressing low levels of B7h. Furthermore, ICOS-Fc downmodulated hepatocyte growth factor facilitated the epithelial-to-mesenchymal transition in HepG2 cells. Moreover, ICOS-Fc downmodulated the phosphorylation of focal adhesion kinase and the expression of β-Pix in both HUVECs and tumor cell lines. Finally, treatment with ICOS-Fc inhibited the development of lung metastases upon injection of NOD-SCID-IL2Rγnull mice with CF-PAC1 cells, as well as C57BL/6 mice with B16-F10 cells. Therefore, the B7h−ICOS interaction may modulate the spread of cancer metastases, which suggests the novel use of ICOS-Fc as an immunomodulatory drug. However, in the B16-F10–metastasized lungs, ICOS-Fc also increased IL-17A/RORc and decreased IL-10/Foxp3 expression, which indicates that it also exerts positive effects on the antitumor immune response. ***The Journal of Immunology*****, 2014, 192: 4921–4931.**

B7 homologoud protein (B7h, also known as B7H2, B7-RP1, ICOSL, GL50, and CD275) belongs to the B7 family of surface receptors and it binds ICOS (CD278), which belongs to the CD28 family (1–9). ICOS is selectively expressed by activated T cells, whereas B7h is expressed by a wide variety of cell types, including B cells, macrophages, dendritic cells (DCs), and a subset of T cells. However, B7h is also expressed by cells of a nonhemopoietic origin such as vascular endothelial cells (ECs), epithelial cells, and fibroblasts, as well as in many primary tumors and tumor cell lines (10–12).

The main known function of B7h is the triggering of ICOS, which functions as a costimulatory molecule for T cells by enhancing their cytokine secretion (3, 13, 14), and in particular, the secretion of IL-10, IL-17, IFN-γ (in humans), IL-4 (in mice), and IL-21 (in both species). The expression of B7h in nonlymphoid tissues, such as the brain, heart, kidney, liver, and intestine, suggests that it regulates the activation of Ag-experienced effector/memory T cells, which are recruited to or reside within these peripheral tissues (15). However, B7h expression also plays a role in secondary lymphoid tissue, particularly in the interaction between T and B cells; ICOS is expressed at high levels by Th follicular cells, and ICOS deficiency has been associated with the defective formation of lymphoid follicles in mice and common variable immunodeficiency in humans (16).

Recent reports have shown that the B7h–ICOS interaction may trigger bidirectional signals that can also modulate the response of the cells expressing B7h. This B7h-mediated "reverse signaling" can induce the partial maturation of immature mouse DCs with augmentation of IL-6 secretion (17). In humans, we have found that B7h triggering via ICOS-Fc, a recombinant soluble form of ICOS, substantially alters DC behavior by modulating the secreted cytokine pattern, which promotes the capacity to cross-present endocytosed Ags in class I MHC molecules and inhibits the adhesiveness to EC

*Department of Drug Science and Technology, University of Torino, 10125 Torino, Italy; †Interdisciplinary Research Center of Autoimmune Diseases, Department of Health Sciences, "A. Avogadro" University of Eastern Piedmont, 28100 Novara, Italy; ‡Department of Molecular Biotechnology and Health Sciences, University of Torino, 10126 Torino, Italy; §Department of Translational Medicine, "A. Avogadro" University of Eastern Piedmont, 28100 Novara, Italy; ¶Department of Microbiology and Immunology, Tokyo Women's Medical University, Tokyo 108-8639, Japan; and ‖Departamento de Medicina Celular y Molecular, Centro de Investigaciones Biologicas, Consejo Superior de Investigaciones Cientıficas, 28006 Madrid, Spain

Received for publication March 1, 2013. Accepted for publication March 11, 2014.

This work was supported by the Associazione Italiana Ricerca sul Cancro (Milan; Grant IG 14430), the Compagnia di San Paolo (Torino), the Fondazione Italiana Sclerosi Multipla (Genoa; Grant 2011/R/11), the Fondazione Amici di Jean (Torino), and the Fondazione Cassa di Risparmio di Cuneo (Cuneo).

C.D. and A.C. performed the functional experiments, analyzed the data, and contributed to writing the manuscript; E.B. and C.L.G. contributed to the cell and tissue preparation, flow cytometry assay, real-time PCR, and analysis; S.O. and L.C. performed the in vivo experiments; R.M., Y.S., and G.C. contributed to the adhesion, migration, and Western blot assays; G.B. performed the epithelial-to-mesenchymal transition and contributed to writing the manuscript; V.M. contributed to the epithelial-to-mesenchymal transition and confocal microscopy assay; D.S. and E.O. prepared the recombinant proteins; R.F., J.Y., M.G., and J.M.R. designed the study and wrote the manuscript; U.D. designed the study, supervised the research, and wrote the manuscript.

Address correspondence and reprint requests to Dr. Annalisa Chiocchetti, Interdisciplinary Research Center of Autoimmune Diseases and Department of Health Sciences, Via Solaroli 17 28100, Novara, Italy. E-mail address: annalisa.chiocchetti@med.unipmn.it

The online version of this article contains supplemental material.

Abbreviations used in this article: DC, dendritic cell; EC, endothelial cell; EMT, epithelial-to-mesenchymal transition; FAK, focal adhesion kinase; HDLEC, human dermal lymphatic endothelial cell; HGF, hepatocyte growth factor; Luc, luciferase; MFI-R, mean fluorescence intensity ratio; NSG, NOD-SCID-IL2Rγnull; Treg, regulatory T cell; VEGF-A, vascular endothelial growth factor-A.

www.jimmunol.org/cgi/doi/10.4049/jimmunol.1300587

and the migratory response to chemoattractants (18). Moreover, we showed that B7h stimulation inhibits the capacity of HUVECs to adhere to several tumor cell lines and granulocytes (11). This inhibitory effect was similarly detected when B7h was triggered on either HUVECs or the tumor cell lines and was accompanied by the decreased phosphorylation of ERK and p38 in HUVECs only. This indicated that the B7h–ICOS interaction modulates the recruitment of granulocytes in inflammatory sites and the spread of cancer metastases from the site of the primary tumor through the bloodstream (11).

The aim of the research reported in this article was to extend these observations by assessing the effect of B7h triggering on other key issues of tumor growth. Tumor growth depends on the proliferation and death rate of the tumor cells, metastasis dissemination depends on their capacity to migrate, and both tumor growth and dissemination are favored by neoangiogenesis within the tumor mass; thus, we assessed the effect of B7h triggering on the proliferation, apoptosis, and migration of tumor cells and vascular ECs. The results showed that B7h triggering strikingly inhibited the migration activity of both tumor and ECs in vitro, which was associated with the dephosphorylation of focal adhesion kinase (FAK) and decreased β-Pix expression. However, B7h triggering had no effect on their proliferation, apoptosis, or the ECs' capacity to form capillary-like structures. Moreover, B7h triggering hampered tumor cell metastasis in vivo.

Materials and Methods

Cells

HUVECs were isolated from human umbilical veins via trypsin treatment (1%) and cultured in M199 medium (Sigma-Aldrich, St. Louis, MO) with the addition of 20% FCS (Invitrogen, Burlington, ON, Canada) and 100 U/ml penicillin, 100 μg/ml streptomycin, 5 UI/ml heparin (Sigma-Aldrich), 12 μg/ml bovine brain extract, and 200 mM glutamine (Hyclone Laboratories, South Logan, UT). HUVECs were grown to confluence in flasks and used at the second to fifth passage. The purity of the ECs preparation was evaluated using morphologic criteria and positive immunofluorescence for factor VIII. Contamination with blood leukocytes was assessed via immunofluorescence with an anti-CD45 Ab. The use of HUVECs was approved by the Ethics Committee of the ''Presidio Ospedaliero Martini'' of Turin and conducted in accordance with the Declaration of Helsinki. Written informed consent was obtained from all donors. Human dermal lymphatic ECs (HDLECs) were purchased from Promo Cell and cultured with Endothelial Cell Growth Medium MV2 (Promo Cell GmbH, Heidelberg, Germany). The following human tumor cell lines were used: HT29, HCT116 (colon adenocarcinoma), PC-3 (prostate carcinoma), CF-PAC1 (human pancreas carcinoma), HepG2 (hepatic carcinoma), and B16-F10 (murine melanoma) from the American Type Culture Collection (ATCC; Manassas, VA); M14, JR8, RPMI7932, PCF-2, and LM (melanoma) from Dr. Pistoia (Gaslini Institute, Genoa, Italy); and BHT-101 (thyroid carcinoma) from Deutche Sammlung von Mikroorganismen and Zellculturen (Braunschweig, Germany). The human tumor cell lines were grown in culture dishes as a monolayer in RPMI 1640 medium (Invitrogen) and DMEM (Invitrogen) for HepG2, CF-PAC1, BHT-101, and B16-F10 plus 10% FCS, 100 U/ml penicillin, and 100 μg/ml streptomycin at 37°C in a 5% CO_2 humidified atmosphere.

The cells were treated or not treated with ICOS-Fc and ^{F119S}ICOS-Fc, in which the extracellular portion of human ICOS and its mutated form carrying a phenylalanine-to-serine substitution at position 119 (^{F119S}ICOS-Fc) were cloned as fusion proteins to the human IgG1 Fc region (11).

The cell-surface phenotypes were assessed via direct immunofluorescence and flow cytometry using the appropriate PE-conjugated anti-B7h mAb (R&D Systems, Minneapolis, MN) and the appropriate FITC-, PE-, and allophycocyanin-conjugated mAb to ICAM-1 (Biolegend, San Diego, CA), ICAM-2 (DiaClone Research, Manchester, U.K.), MadCAM (Abcam, Cambridge, MA), CD31, CD62L, CD62E, CD62P (Immunotools, Friesoythe, Germany), $CD44v_{6-7}$ (Bender Med-Systems, Vienna, Austria), Sialyl Lewis X (Santa Cruz Biotechnology, Dallas, TX), and VCAM-1 (eBiosciences, San Diego, CA). The expression of Sialyl Lewis A was assessed via indirect immunofluorescence using an appropriate mAb (Santa Cruz Biotechnology) and FITC-conjugated goat anti-mouse Ig (Caltag Laboratories, Burlingame, CA). The mean fluorescence intensity ratio (MFI-R) was calculated considering all of the alive cells according to the following formula: MFI of the B7h-stained sample histogram (arbitrary units)/MFI of the control histogram (arbitrary units). The B16-F10 cells were split into two cell lines expressing high or low levels of B7h ($B7h^{high}$ and $B7h^{low}$) via magnetic selection with PE-conjugated anti-B7h mAb and anti-PE microbeads (Miltenyi Biotec, Bergisch Gladbach, Germany).

Cell growth assays

In the MTT assay, the cells were normalized at 800 or 2500 cells/100 μl in 96-well plates for HT29 or HUVECs, respectively. After an overnight incubation, the medium was replaced with 100 μl culture medium with 0.5–4 μg/ml ICOS-Fc. In some experiments, the cells were refilled every 24 h with 4 μg/ml ICOS-Fc. After 24, 48, and 72 h of incubation, the viable cells were detected via MTT (Sigma-Aldrich) at 570 nm, as described by the manufacturer's protocol. The absorbance of the controls (i.e., the cells that received no drug) was normalized to 100%, and that of the ICOS-Fc–treated cells was expressed as the percentage of the controls. Eight replicate wells were used to determine each data point, and three different experiments were performed.

In the colony-forming assay, cells (800/well) were seeded into six-well plates and treated with the compounds. The medium was changed after 72 h, and the cells were cultured for another 10 d. Subsequently, the cells were fixed and stained with a solution of 80% crystal violet (Sigma-Aldrich) and 20% methanol (Sigma-Aldrich). The colonies were then photographed and counted with Gel Doc equipment (Bio-Rad Laboratories, Hercules, CA).

In the cell death assay, the cells were incubated with and without either etoposide (2 μg/ml; Sigma-Aldrich) or FCS for 18 h, and cell death was then evaluated by counting the live cells with the trypan blue exclusion test and detecting the dead cells upon cytofluorimetric analysis of the cells stained with FITC-conjugated Annexin V (BD Biosciences, San Jose, CA) and propidium iodide (Sigma-Aldrich).

Cell migration assays

In the Boyden chamber (BD Biosciences) migration assay, cells (8000) were plated onto the apical side of 50 μg/ml Matrigel-coated filters (8.2-mm diameter and 0.5-μm pore size; Neuro Probe; BIOMAP snc, Milan, Italy) in serum-free medium with or without 2 μg/ml ICOS-Fc or ^{F119S}ICOS-Fc. Medium containing either 20% FCS or 10 ng/ml vascular endothelial growth factor-A (VEGF-A; Sigma-Aldrich) or 50 ng/ml hepatocyte growth factor (HGF; PeproTech, Rocky Hill, CT) was placed in the basolateral chamber as a chemoattractant for the tumor, endothelial, or HepG2 cells, respectively. The chamber was incubated at 37°C under 5% CO_2. After 8 h, the cells on the apical side were wiped off with Q-tips. The cells on the bottom of the filter were stained with crystal violet and counted (five fields for each triplicate filter) with an inverted microscope (magnification ×100). The results are expressed as the number of migrated cells per high-power field.

In the wound-healing experiments, the cells were plated onto six-well plates (at a concentration of 10^6 cells/well) and grown to confluence. The cells were then left for 12 h with FCS-free medium (to prevent cell proliferation). The cell monolayers were carefully wounded by scratching with a sterile plastic pipette tip along the diameter of the well. The cells were washed twice with FCS-free medium and then incubated with culture medium in the absence or presence of 2 μg/ml ICOS-Fc. Five fields of each of the three wounds analyzed per condition were photographed immediately after the scratch had been made (0 h) and 24 h later to monitor cell movement into the wounded area.

In the cell scatter assay, the cells were plated on 24-well plates (2×10^4/well HepG2, 3×10^4/well BHT-101) in 10% FCS and stimulated with the indicated treatments. Phase-contrast images of random fields were acquired (after 48 h for HepG2 and 24 h for BHT-101) with an Axiovert 40 CFL microscope (Zeiss, Oberkochen, Germany) and analyzed with Image-Pro-Plus software. For each experimental point, the length of at least 100 cells and the percentage of disaggregated single cells were evaluated in 3 separate images. For confocal microscopy, the cells were washed with PBS and fixed in PBS containing 3% paraformaldehyde and 4% sucrose. The cells were permeabilized in cold HEPES-Triton buffer (20 mM HEPES, 300 mM sucrose, 50 mM NaCl, 3 mM MgCl2, 0.5% Triton X-100, pH 7.4). Intermediate washing was performed with PBS containing 0.2% BSA. PBS containing 2% BSA (Sigma-Aldrich) was used as a blocking reagent. Alexa Fluor 546 Phalloidin (Invitrogen) and TO-PRO3 (Invitrogen) were diluted in 2% PBS-BSA and added directly onto each glass coverslip in a humidified chamber for 30 min. Finally, each glass coverslip was washed briefly in water and mounted onto a glass microscope slide using Mowiol resin (Sigma-Aldrich, 20% Mowiol 4-88, 2.5% 1,4-diazabicyclo[2.2.2]octane in PBS, pH 7.4). Confocal images were acquired with a Leica confocal microscope TCS SP2 equipped with LCS Leica confocal software (63× objective for HepG2

or 40× objective for BHT-101; Leica Microsystems, Wetzlar, Germany). Basal planes are shown.

Angiogenesis assays

In the tube-formation assay, HUVEC cells were seeded onto 24-well plates (5×10^4/well) previously coated with 150 μl growth factor–reduced Matrigel (BD Biosciences) in the presence of ICOS-Fc (2–4 μg/ml) or control medium. The morphology of the capillary-like structures formed by the HUVECs was analyzed after 15 h of culture using an inverted microscope and was photographed with a digital camera. Tube formation was analyzed with an imaging system (Image-Pro).

In the spheroid sprouting assay, ECs were coated onto Cytodex microcarriers and embedded in a fibrin gel. Factor X, which was extracted from confluent fibroblasts medium, was added to the medium to promote ECs sprouting from the surface of the beads. After 4–5 d, numerous vessels could be observed with a phase-contrast microscope. The newly formed vessels were then treated or not treated with ICOS-Fc (4 μg/ml), and vessel morphology was analyzed 5 d later.

Western blot analysis

The cells were lysed in a buffer composed of 50 mM Tris-HCl pH 7.4, 150 mM NaCl, 5 mM EDTA, 1% nonyl phenoxypolyethoxylethanol 40, and phosphatase and protease inhibitor cocktails (P2850, P8340; Sigma-Aldrich). The tissues were lysed in a buffer composed of 160 mM NaCl, 20 mM Tris-HCl pH 7.4, 1 mM EDTA, 1 mM EGTA, 1% Triton X-100, 1% sodium deoxycholate, and 0.1% SDS. The lysates were then cleared of insoluble fractions through high-speed centrifugation, and the protein concentrations were determined with a commercially available kit (Bio-Rad Laboratories). Then 40 μg proteins were loaded on 10% SDS PAGE gels, and after electrophoresis, transferred onto Hybond-C extra nitrocellulose membranes (Ge Healthcare, Piscataway, NJ). These were blocked for 1 h at room temperature with 5% nonfat milk dissolved in TBST. The membranes were then probed overnight with Abs to β-Pix (SH3 domain; Millipore, Billerica, MA), phospho-FAK (Y397; Cell Signaling Technology, Danvers, MA), FAK (BD Biosciences), β-actin (A1978; Sigma-Aldrich), and after 3 washes, incubated for 1 h with HRP-conjugated secondary Abs (GE Healthcare, Piscataway, NJ). The bands were detected via chemiluminescence, and densitometric analysis was performed using Multi-Analyst software (version 1.1; Bio-Rad Laboratories).

In vivo experiments

Female 4- to 5-wk-old NOD-SCID-IL2Rγnull (NSG; The Jackson Laboratory, Bar Harbor, ME) mice were bred under pathogen-free conditions in the animal facility of the Molecular Biotechnology Center, University of Turin, and were treated in accordance with the University Ethical Committee and European guidelines. The mice were injected in the tail vein with stably expressing firefly luciferase (Luc) CF-PAC1 (human pancreas carcinoma) cells (0.5×10^6/mouse) and monitored for pulmonary metastases after 3 d via in vivo optical imaging. In each experiment, the mice were treated every day via the i.p. injection of either human ICOS-Fc plus mouse ICOS-Fc, human ICOS-Fc alone, mouse ICOS-Fc alone, human ^{F119S}ICOS-Fc alone (100 μg each), or the same volume of PBS as a control. Three days after tumor cell injection, the mice were injected i.p. with 150 mg/Kg luciferin (Perkin Elmer, Waltham, MA) in sterile PBS. They were then placed in the IVIS 200 (Perkin Elmer) induction chamber and subjected to inhalational isoflurane anesthesia (Abbott, Abbott Park, IL) at 2.5% with 1 l/min flow of oxygen. After 10 min, the mice were placed on the heated imaging platform of the IVIS 200 imaging station with inhalational isoflurane anesthesia during the imaging procedure. White light and Luc activity images were acquired with a 25-s exposure. The images

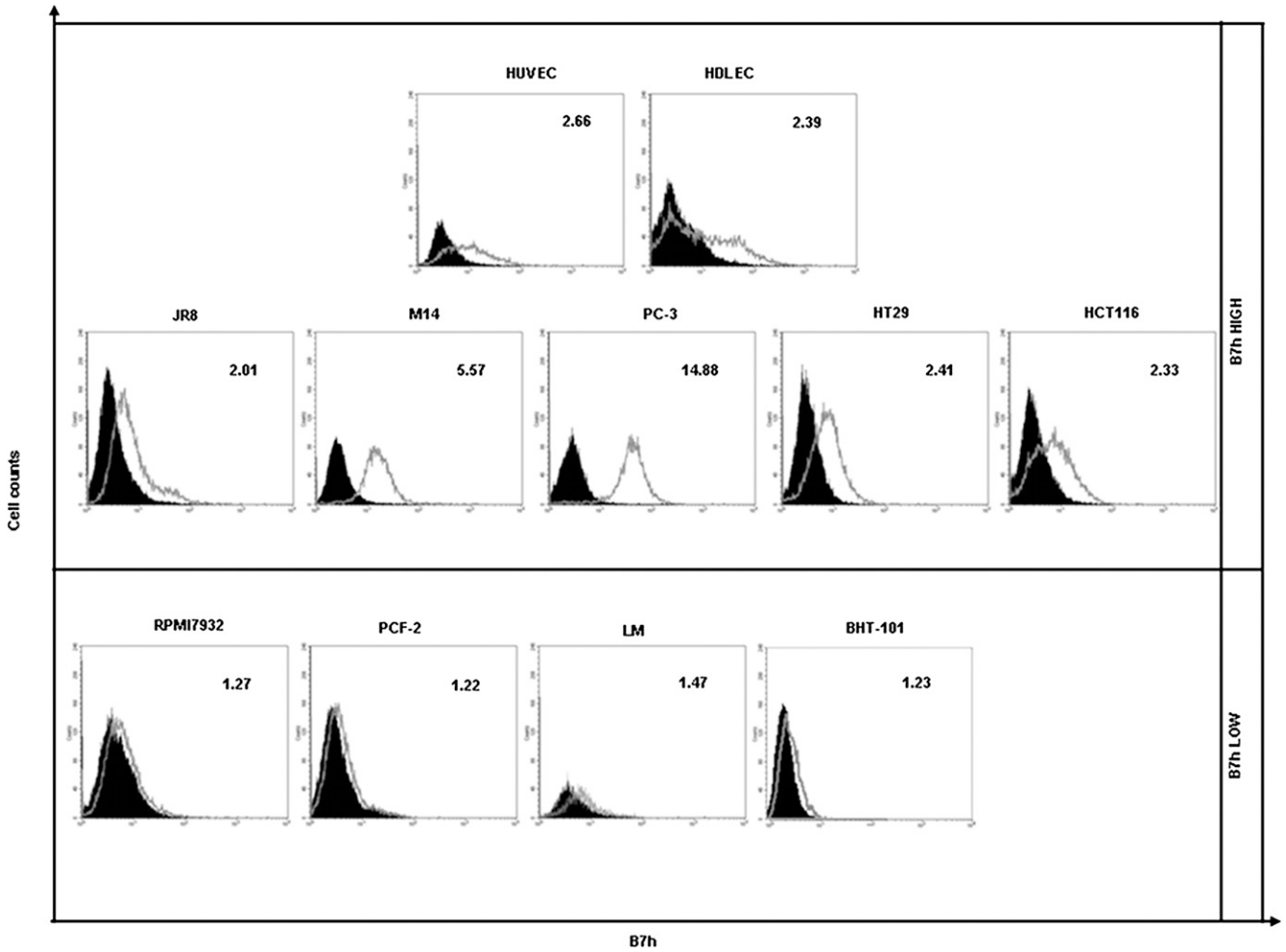

FIGURE 1. B7h expression in endothelial and tumor cell lines. B7h expression was assessed in the HUVEC, HDLEC, JR8, M14, PC-3, HT29, HCT116, RPMI7932, PCF-2, LM, and BHT-101 cell lines via flow cytometry using an anti-B7h mAb. The numbers in each panel indicate the MFI-R. The cutoff between the $B7h^{high}$ and $B7h^{low}$ cells was set at MFI-R = 2.

were analyzed with the Living Image software (PerkinElmer). The luminescent signal was quantified as the average radiance (p/s/cm^2/sr) measured in the regions of interest drawn in the lungs.

Female 5- to 7-wk-old C57BL/6 mice (Harlan Laboratories, Indianapolis, IN) were injected in the tail vein with B7h^{high} B16-F10 cells (10^6 cells/mouse) and then treated daily with an i.p. injection of either the mouse ICOS-Fc, the human ^{F119S}ICOS-Fc (100 μg each), or the same volume of PBS as a control. Two weeks after cell injection, the mice were euthanized, and the number of metastases detectable in the lung surfaces was evaluated by two blinded observers. In some experiments, the mice were euthanized 3 d after cell injection, and the metastases were counted in fixed sections of the lungs stained with H&E (Sigma-Aldrich).

The infiltrating cells were obtained by grinding the fresh lungs, obtained at day 3, through a 100-μm cell strainer mesh (BD Biosciences); the total RNA was then isolated using TRIzol reagent (Invitrogen). RNA (500 ng) was retrotranscribed using the ThermoScript RT PCR System (Invitrogen). IL-17A, IL-10, IL-21, RORc, Foxp3, and Bcl6 expression were evaluated with a gene expression assay (Assay-on Demand; Applied Biosystems, Foster City, CA). The β-glucuronidase gene was used to normalize the cDNA amounts. Real-time PCR was performed using the CFX96 System (Bio-Rad Laboratories) in duplicate for each sample in a 10 μl final volume containing 1 μl diluted cDNA, 5 μl TaqMan Universal PCR Master Mix (Applied Biosystems), and 0.5 μl Assay-on Demand mix. The results were analyzed with a Δ-Δ threshold cycle method.

In other experiments, the C57BL/6 mice were injected s.c. with 10^6B7h^{high} B16-F10 cells. When the tumor diameter reached 4 mm, the mice received an intratumoral injection of the mouse ICOS-Fc, human^{F119S}ICOS-Fc (100 μg each), or the same volume of PBS as a control. After 30 min, the tumors were excised and immediately frozen in liquid nitrogen for Western blot analyses.

Data analysis

The data are shown as the mean ± SEM. The statistical analyses were performed with GraphPad Prism 3.0 software using one-way ANOVA and Dunnett's test (GraphPad Software, San Diego, CA).

Results

B7h triggering has no effect on cell proliferation and apoptosis

To assess the effect of B7h triggering (via ICOS-Fc) on the proliferation, apoptosis, and migration of the tumor cells and vascular ECs, we used two primary EC lines (HUVECs and HDLECs) and nine continuous tumor cell lines (HT29 and HCT116 [colon carcinoma], PC-3 [prostate carcinoma], M14, JR8, RPMI7932, PCF-2, LM [melanoma], and BHT-101 cells [thyroid carcinoma]). The surface immunofluorescence and flow cytometry showed that B7h was expressed in all cell lines and at high levels (B7h^{high}) in HUVECs, HDLECs, JR8, M14, PC-3, HT29, and HCT116, but low levels (B7h^{low}) in BHT-101, RPMI7932, PCF-2, and LM (Fig. 1).

Initially, the effect of ICOS-Fc on cell proliferation and death was assessed in HUVECs, HT29, and PC-3, which expressed high levels of B7h. In the proliferation assay, the cells were cultured in the presence of various concentrations of ICOS-Fc (0.5–4 μg/ml) for 24–96 h, and cell proliferation was then assessed via the MTT and the clonogenic assays. The results showed that ICOS-Fc did not modulate cell proliferation in any cell line at any dose or time

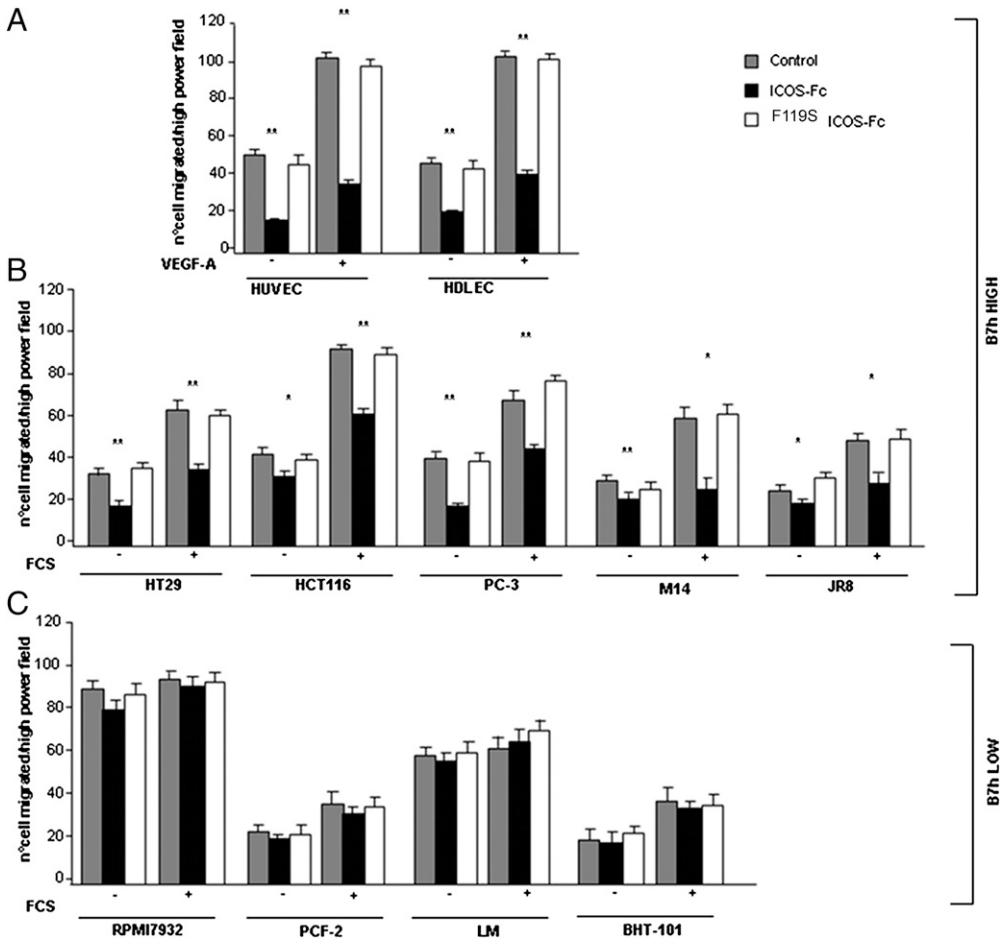

FIGURE 2. The effect of ICOS-Fc on the motility of the endothelial and tumor cell lines as assessed via a Boyden chamber assay. Cells: (**A**) HUVEC and HDLEC; (**B**) HT29, HCT116, PC-3, M14, and JR8; (**C**) RPMI7932, PCF-2, LM, and BHT-101 were plated onto the apical side of Matrigel-coated filters in 50 μl medium in the presence or absence of either 2 μg/ml ICOS-Fc or ^{F119S}ICOS-Fc; either VEGF-A (10 ng/ml) or 20% FCS was loaded in the basolateral chamber as chemotactic stimulus. The cells that migrated to the bottom of the filters were stained using crystal violet and counted (five fields for each triplicate filter) using an inverted microscope. The data are expressed as the mean ± SEM ($n = 5$) of the number of migrated cells per high-power field (*$p < 0.05$, **$p < 0.01$ versus the control).

(data not shown), even when the ICOS-Fc was refilled every 24 h. In the cell death assay, the cells were cultured for 18 h in the presence or absence of ICOS-Fc (2 μg/ml) either in the absence of FCS (to induce cell death by neglect) or in the presence of etoposide. Then cell survival was assessed after 18 h by counting the surviving cells with the trypan blue exclusion test, and the dead cells were evaluated by staining with propidium iodide and FITC-conjugated Annexin V followed by cytofluorimetric analysis. The results showed that ICOS-Fc did not induce cell death and did not modulate either cell death by neglect or that induced by etoposide in any cell line (data not shown).

B7h triggering inhibits cell migration and the epithelial-to-mesenchymal transition

To evaluate the effect of ICOS-Fc on cell migration, we seeded the endothelial and the tumor cell lines in the upper chamber of a Boyden chamber in serum-free medium in the presence or absence of ICOS-Fc (2 μg/ml) and allowed them to migrate for 8 h toward the lower chamber containing medium supplemented or not supplemented with either VEGF-A (10 ng/ml) or 20% FCS, which were used as chemoattractants for the endothelial and the tumor cells, respectively. As a control, the same experiments were performed in the presence of ^{F119S}ICOS-Fc, a mutated form of ICOS-Fc carrying a phenylalanine-to-serine amino acid substitution at position 119 that is unable to bind B7h. The results showed that ICOS-Fc significantly inhibited cell migration by ~50–70% in all of the B7h^{high} cell lines (i.e., HUVECs, HDLECs, HT29, HCT116, PC-3, M14, and JR8) in both the presence and the absence of the chemoattractants (Fig. 2A, 2B). This effect was specific because it was not exerted by ^{F119S}ICOS-Fc. In contrast, neither ICOS-Fc nor ^{F119S}ICOS-Fc exerted any effect on the B7h^{low} cell lines (i.e., RPMI7932, PCF-2, LM, and BHT-101), which indicated that the inhibitory effect was B7h mediated (Fig. 2C).

To confirm the effect of ICOS-Fc on directional cell migration, we performed the scratch assay, an in vitro "wound healing" assay, on PC-3, HT29, and HUVECs, because cell migration is highly efficient for PC-3, poor for HT29, and intermediate for HUVECs in this assay. A linear scratch was performed on a confluent monolayer of each cell line, and they were then cultured in FCS-free medium to minimize cell proliferation in the presence or absence of ICOS-Fc (2 μg/ml). A microscopic analysis evaluating cell capacity to migrate and fill the empty areas at different times showed that in the absence of ICOS-Fc, substantial cell migration was detectable in the wound area for PC-3 and HUVECs, and that it was substantially inhibited by ICOS-Fc (Fig. 3). This inhibition was also detectable for HT29 cells, which displayed a low migratory activity that was detectable as a fringing of the scratch edges after the 24-h incubation; this pattern was substantially inhibited by ICOS-Fc.

To assess the effect of ICOS-Fc on the epithelial-to-mesenchymal transition (EMT), we performed a scatter assay to treat the HepG2 cells (hepatic carcinoma) with HGF. In cultures, these cells grow as colonies that maintain an epithelial morphology; however, they break down cell junctions and acquire an elongated mesenchymal phenotype upon HGF/scatter factor treatment (19). A cytofluorimetric analysis showed that these cells express high levels of B7h (Fig. 4A). The cells were treated for 72 h in 10% FCS with or without HGF (50 ng/ml) and in the presence or absence of either ICOS-Fc (2 μg/ml) or ^{F119}ICOS-Fc (2 μg/ml). They were then directly analyzed via phase-contrast microscopy (Fig. 4B, *left panel*) or stained with Alexa Fluor 546 Phalloidin and imaged via confocal microscopy (Fig. 4B, *right panel*). The results showed that ICOS-Fc substantially inhibited the cell scatter induced by HGF by

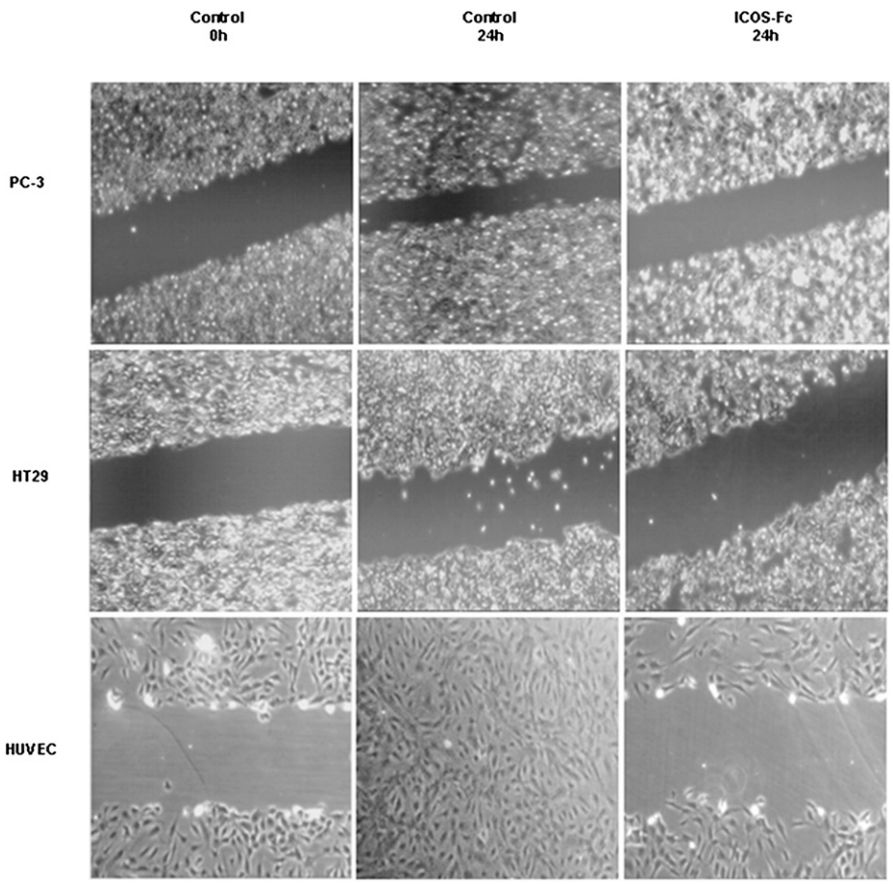

FIGURE 3. Effect of ICOS-Fc on the motility of the PC-3, HT29, and HUVECs as assessed using a "wound-healing" assay. The cells were grown to confluence on six-well plates. A scratch was made through the cell layer using a pipette tip; the cells were washed and then cultured in the presence or absence of 2 μg/ml ICOS-Fc for 24 h. Microphotographs of the wounded area were taken immediately after the scratch was made (0 h) and 24 h later to monitor cell migration into the wounded area (original magnification ×10). Panels show a representative experiment from three experiments.

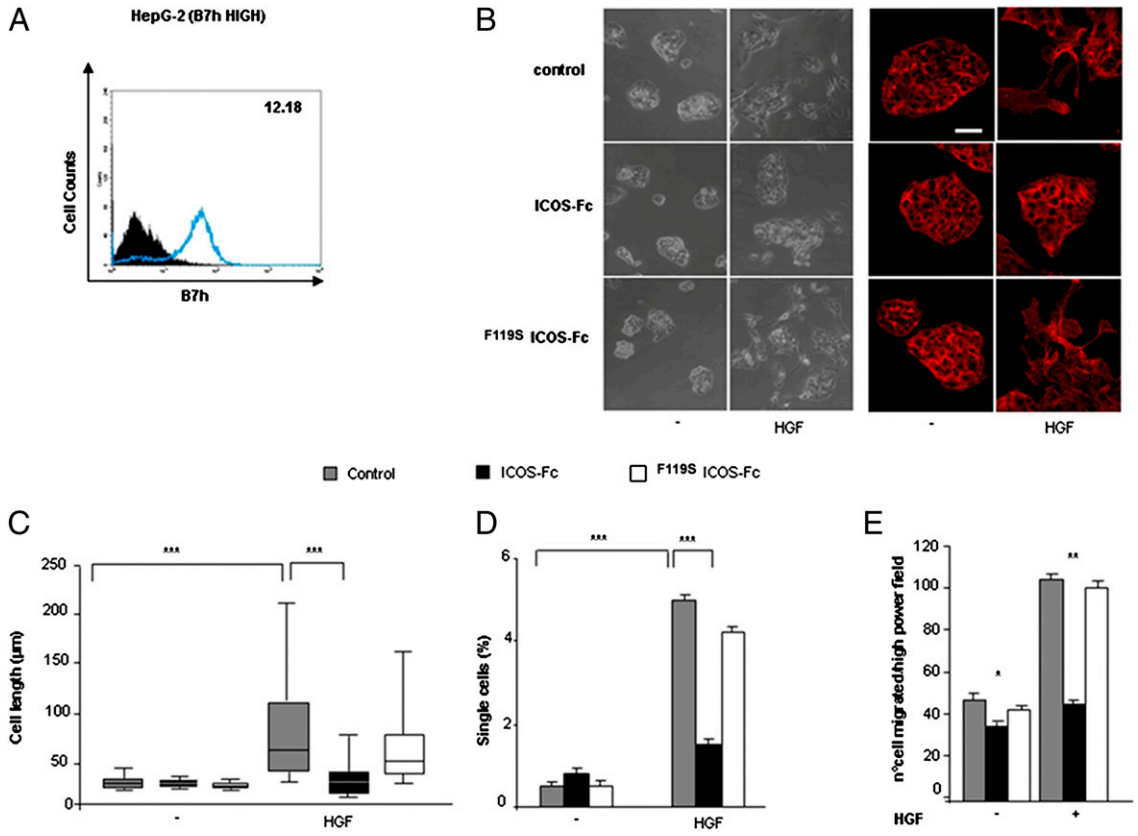

FIGURE 4. ICOS-Fc impairs HGF-induced cell scatter in HepG2 cells. (**A**) Cytofluorimetric analysis of the B7h expression in the HepG2 cells (performed as in Fig. 1). The HepG2 cells were treated for 48 h in 10% FCS with or without HGF (50 ng/ml), ICOS-Fc (2 μg/ml), or ^{F119S}ICOS-Fc (2 μg/ml). (**B**) The cells were photographed via phase contrast (*left panel*) or stained with Alexa Fluor 546 Phalloidin and imaged via confocal microscopy (*right panel*). Scale bar, 40 μm. (**C**) Whisker plot showing the cell length (excluding the outliers of a representative experiment). (**D**) Percentage of the disaggregated single cells (mean ± SEM of 4 experiments); at least 100 cells were counted for each point. (**E**) Effect of ICOS-Fc on the migration of HepG2 cells treated with HGF in the Boyden chamber assay (performed as in Fig. 2). $*p < 0.05$, $**p < 0.01$, $***p < 0.001$.

impairing the acquisition of the elongated mesenchymal morphology (median length of ICOS-Fc–untreated versus –treated cells: 60 mm versus 31 mm; Fig. 4C) and promoting the maintenance of colonies with cell-to-cell junctions and smooth borders with decreased numbers of disaggregated single cells (Fig. 4D). We also assessed the effect of ICOS-Fc on the migration of HepG2 cells induced by HGF (50 ng/ml) in the Boyden chamber assay. In accordance with the previous results, ICOS-Fc, but not ^{F119S}ICOS-Fc, inhibited the stimulated migration of HepG2 by ~50% (Fig. 4E). To assess whether these effects were dependent on B7h expression, we evaluated the effect of ICOS-Fc and ^{F119S}ICOS-Fc on the HGF-induced cell scattering of BHT-101, which was previously shown to express low levels of B7h (Fig. 1) and to display no ICOS-Fc–induced migration inhibition (Fig. 2). Because these cells showed modest elongation upon HGF treatment, their scattering was quantified only by counting the percentage of disaggregated single cells. The results showed that neither ICOS-Fc nor ^{F119S}ICOS-Fc inhibited BHT-101 cell scattering (Supplemental Fig. 1).

B7h triggering has no effect on angiogenesis

To assess the effect of B7h triggering on angiogenesis, we evaluated the effect of ICOS-Fc via the endothelial tube-formation assay and the spheroid sprouting assay. In the tube-formation assay, HUVECs were seeded onto 24-well plates (5×10^4/well) previously coated with 150 μl growth factor–reduced Matrigel in the presence of ICOS-Fc (2–4 μg/ml) or control medium. The morphology of capillary-like structures formed by HUVECs was analyzed 15 h after culturing. The results showed that ICOS-Fc did not significantly affect tube formation in HUVECs (data not shown).

In the spheroid sprouting assay, ECs were coated onto Cytodex microcarriers and embedded in a fibrin gel in the presence of factor X to promote EC sprouting from the surface of the beads. After 4–5 d, the newly formed vessels were treated or not treated with ICOS-Fc (4 μg/ml); vessel morphology was analyzed 5 d later. The results showed that ICOS-Fc did not significantly affect vessel caliper or length (data not shown).

B7h triggering inhibits β-Pix expression and FAK phosphorylation

To assess whether treatment with ICOS-Fc modulated the expression of adhesion molecules, we analyzed the surface expression of ICAM-1, ICAM-2, MadCAM, CD62P, CD31, CD44v_{6-7}, CD62E, Sialyl Lewis A, CD62L, VCAM-1, and Sialyl Lewis X via immunofluorescence and flow cytometry in JR8, M14, and HT-29 cells treated or untreated with ICOS-Fc for 30 min, 1, 4, and 24 h. The results showed that ICOS-Fc did not modulate the expression of any of these molecules (data not shown), which is in accordance with previous data obtained for HUVECs and DCs (11, 18).

In previous studies, we have shown that B7h triggering inhibits the phosphorylation of p38 and ERK induced by either E-selectin triggering or osteopontin in HUVECs (this occurred without affecting their basal phosphorylation), whereas no effect was detected in the tumor cell lines (11). Moreover, we showed that in

DCs, B7h inhibits the expression of the Rac-1 activator β-Pix, which is involved in cell motility (18). Therefore, we evaluated the effect of ICOS-Fc on the β-Pix expression in two B7h^{high} cell lines (PC-3, HUVECs) and two B7h^{low} cell lines (RPMI7932, BHT-101), and extended the analysis to the phosphorylation of FAK, involved in cell migration. The cells were either not treated or were treated with ICOS-Fc or ^{F119S}ICOS-Fc; β-Pix expression and FAK phosphorylation were then assessed via Western blot after 30 min. The results showed that ICOS-Fc substantially decreased β-Pix expression and FAK phosphorylation in the B7h^{high} cell lines (Fig. 5A, 5B), whereas no effect was detected in the B7h^{low} cell lines (Fig. 5C, 5D). The treatment with ^{F119S}ICOS-Fc showed no effect for any cell line.

B7h triggering inhibits tumor cell metastasis in vivo

The effect of B7h triggering on the metastasis capability in vivo was assessed by injecting NSG mice with CF-PAC1 Luc cells (human pancreas carcinoma). A previous in vitro analysis showed that this cell line expresses high levels of B7h (Fig. 6A) and that its treatment with ICOS-Fc, but not with ^{F119S}ICOS-Fc, inhibits migration in the Boyden chamber assay (Fig. 6B), as well as β-Pix expression and FAK phosphorylation (Fig. 6C); these findings are in accordance with the data obtained for the other B7h^{high} cell lines.

NSG mice were i.v. injected with 0.5×10^6 CF-PAC1 Luc cells and then i.p. treated with both the human and the mouse ICOS-Fc ($n = 7$) or PBS ($n = 7$) every day to trigger both the B7h expressed by the human tumor cell line and that expressed by the mouse vascular ECs; this treatment would mimic the putative effect of the human ICOS-Fc injected in humans. Three days after cell injection, the mice were i.p. injected with luciferin and analyzed via in vivo optical imaging to evaluate the tumor cell growth in the lung. Qualitative (Fig. 6D) and quantitative (Fig. 6E) analyses showed that a significantly higher luminescent signal was present in control mice than in those treated with ICOS-Fc. To determine whether this effect was due to the human or mouse ICOS-Fc, we repeated these experiments by treating the mice with either the human ICOS-Fc alone ($n = 3$), the mouse ICOS-Fc alone ($n = 3$), the human ^{F119S}ICOS-Fc alone ($n = 3$), or PBS ($n = 3$). The qualitative (Fig. 6F) and quantitative (Fig. 6G) analyses showed that a significantly higher luminescent signal was present in the control mice and those treated with ^{F119S}ICOS-Fc than in mice treated with either the human or mouse ICOS-Fc alone. In contrast, no significant differences were detected between the control mice and those treated with ^{F119S}ICOS-Fc.

To confirm these data, we assessed the ICOS-Fc effect on the metastasis of B16-F10 cells (mouse melanoma) in C57BL/6 mice. In a preliminary experiment, we separated the B7h^{high} and B7h^{low} B16-F10 cells using magnetic beads and found that these cell lines maintained their phenotype for several weeks in culture. Moreover, treatment with ICOS-Fc, but not with ^{F119S}ICOS-Fc, inhibited migration in Boyden chamber assay, as well as β-Pix expression and FAK phosphorylation in the B7h^{high} cell line, whereas no effects were detected in the B7h^{low} cell line (Supplementary Fig. 2).

The C57BL/6 mice were i.v. injected with 10^6 B7h^{high} B16-F10 cells and then i.p. treated with either the mouse ICOS-Fc ($n = 3$), human ^{F119S}ICOS-Fc ($n = 3$), or PBS ($n = 3$) every day. The lung metastases were analyzed either after 3 d (for the tissue sections stained with H&E) or after 2 wk by counting the tumor nodules

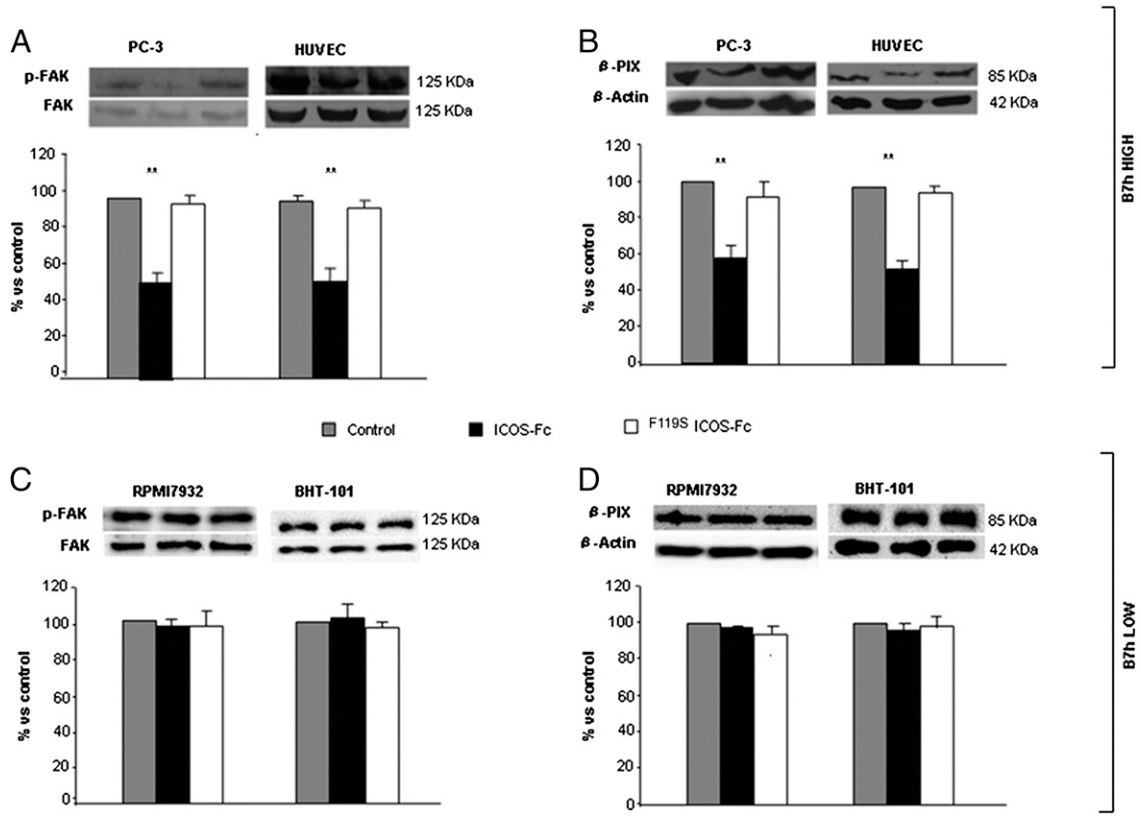

FIGURE 5. Effect of ICOS-Fc on FAK phosphorylation and β-Pix expression in the B7h^{high} (PC-3, HUVEC) and B7^{low} (RPMI7932, BHT-101) cell lines. The cell lines were treated with 4 μg/ml ICOS-Fc or ^{F119S}ICOS-Fc for 30 min; p-FAK (**A** and **C**) and β-Pix (**B** and **D**) expression were then evaluated via Western blot in the cell lysates. The same blots were also probed with anti-FAK or anti–β-actin Ab as a control. The bar graphs show the densitometric analysis of the gels expressed in arbitrary units; data are expressed as the mean ± SEM of the percentage of inhibition versus the control from three independent experiments (**$p < 0.01$ versus the control).

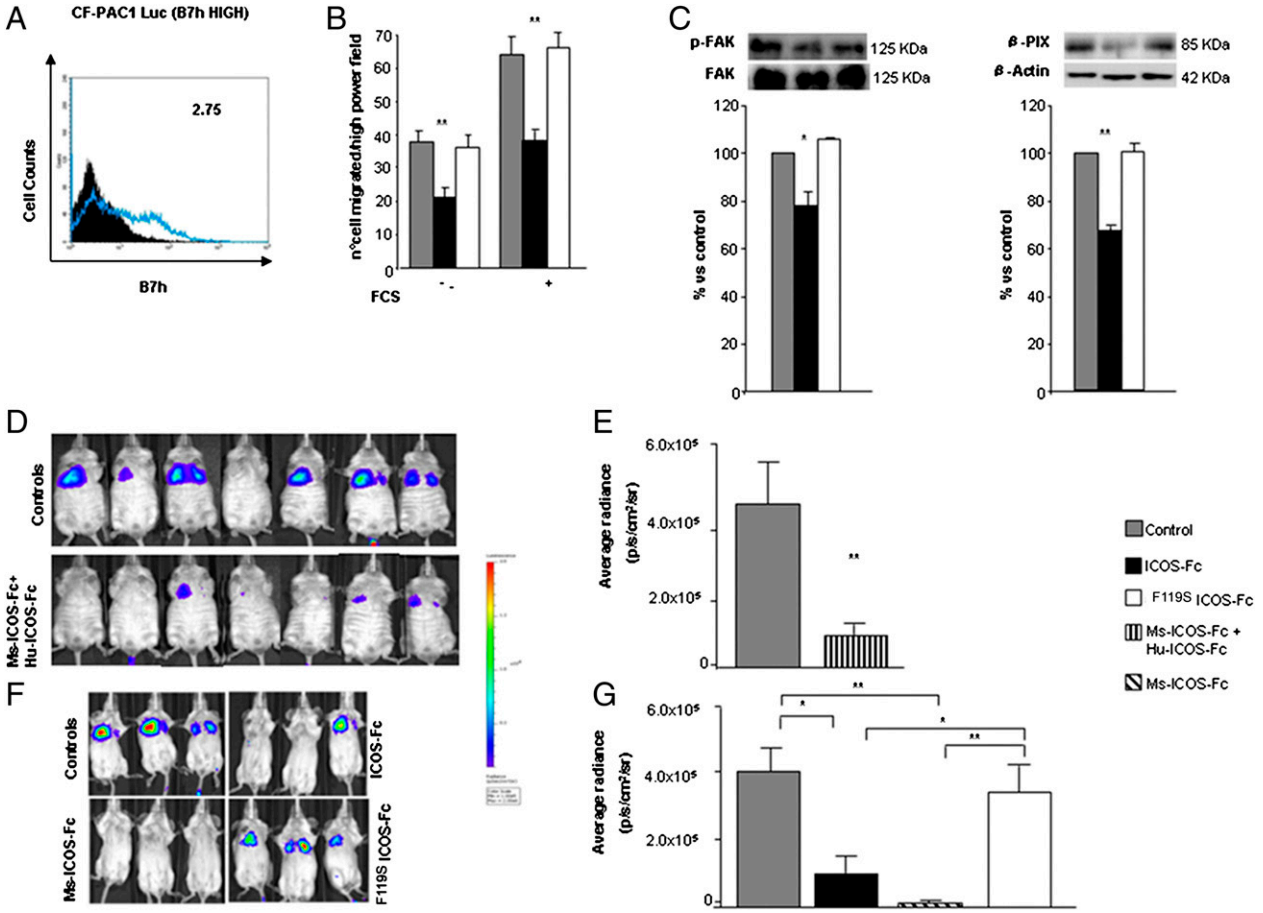

FIGURE 6. Effects of B7h triggering on CF-PAC1 tumor cell metastasis in vivo. (**A**) Cytofluorimetric analysis of B7h expression in the CF-PAC1 Luc cells (performed as in Fig. 1). (**B**) Effect of ICOS-Fc on the migration of the CF-PAC1 Luc cells in the Boyden chamber assay (performed as in Fig. 2). (**C**) Effect of ICOS-Fc on the expression of p-FAK and β-Pix (performed as in Fig. 5). (**D** and **E**) Mice were injected i.v. with 0.5×10^6 CF-PAC1 Luc cells and treated with the human ICOS-Fc plus mouse ICOS-Fc ($n = 7$) or PBS (control group, $n = 7$). (**F** and **G**) The mice injected with CF-PAC1 Luc were treated with either the human ICOS-Fc ($n = 3$), mouse ICOS-Fc ($n = 3$), human ^{F119S}ICOS-Fc ($n = 3$), or PBS (control group, $n = 3$). After 3 d, the mice were i.p. injected with luciferin, and pulmonary metastases were macroscopically detectable and documented via in vivo optical imaging. The luminescent signal was quantified as the average radiance (p/s/cm^2/sr), which was measured in regions of interest drawn in the lungs. Data are expressed as the mean ± SEM and were obtained in two independent experiments ($*p < 0.05$, $**p < 0.01$).

detectable on the lung surface. Both approaches showed that the mice treated with the mouse ICOS-Fc displayed significantly fewer metastases than those treated with either PBS or the human ^{F119S}ICOS-Fc (Fig. 7A, 7B). To determine whether the treatments modulated the immune response, we obtained infiltrating cells from the lungs, and we evaluated the mRNA levels of IL-17A and RORc (marking Th17 cells), IL-10 and Foxp3 (marking regulatory T cells [Tregs]), and IL-21 and Bcl6 (marking T follicular helper cells) via real-time PCR (because ICOS has a key role in Th17, Treg, and T follicular helper cell function) (3, 13–15). The results showed that treatment with the mouse ICOS-Fc significantly increased the expression of IL-17A and RORc, and decreased that of IL-10 and Foxp3 compared with the levels detected in control mice and those treated with the human ^{F119S}ICOS-Fc (Fig. 7C). In contrast, no differences were detected in the expression of Bcl6, whereas IL-21 was always undetectable (data not shown). Moreover, ICOS-Fc did not modulate the expression of these molecules in the control mice not injected with the B16-F10 cells; in these mice, Foxp3 and Bcl6 were expressed at low levels, whereas IL-17A, RORc, IL-10, and IL-21 were undetectable (data not shown).

To assess whether treatment with ICOS-Fc decreased β-Pix expression and FAK phosphorylation in vivo, the C57BL/6 mice were injected s.c. with 10^6 B7h^{high} B16-F10 cells. When the tumor diameter reached 4 mm, the mice received one intratumor injection of either the mouse ICOS-Fc, human ^{F119S}ICOS-Fc, or the same volume of PBS. After 30 min, the tumors were excised, and β-Pix expression and FAK phosphorylation were assessed in the tissue lysates via Western blot. The results showed that treatment with ICOS-Fc, but not with ^{F119S}ICOS-Fc, substantially decreased the expression of β-Pix compared with that detected in the control mice (Fig. 7D). The FAK expression was similar in all conditions, and the phospho-FAK expression was always undetectable (data not shown).

Discussion

Cancer progression involves a complex interplay between the tumor and the microenvironment that results in sustained proliferative signaling, resistance to cell death, as well as the promotion of angiogenesis, invasion, and metastasis (20–23). This work has shown that ICOS binding to B7h influences several of these events by acting on both ECs and tumor cells. These effects were specific; they were not displayed by a mutated form of ICOS-Fc that was incapable of binding B7h.

The most striking effect was that on tumor cells: ICOS-Fc inhibited EMT and migration in vitro, as well as metastasis in vivo. EMT is a transdifferentiation program required for tissue morphogenesis during the embryonic development; its induction is exploited by cancer cells to acquire invasive and metastatic properties. Recent

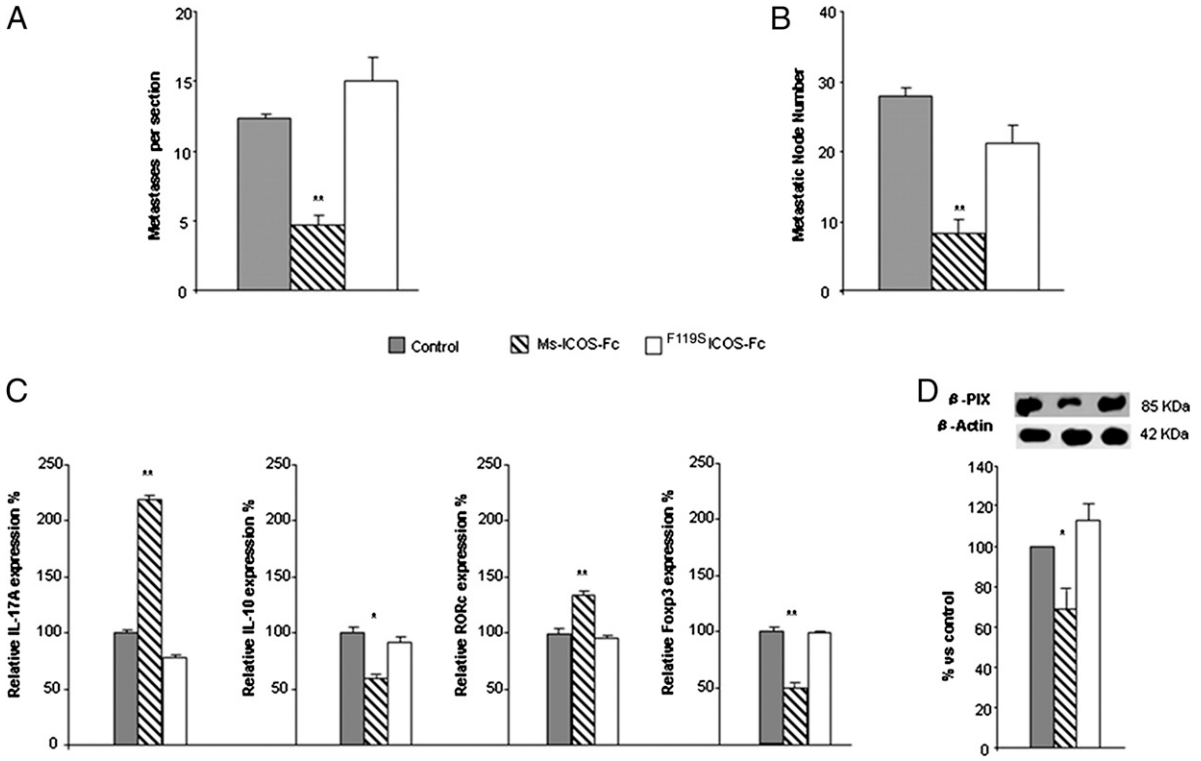

FIGURE 7. Effect of B7h triggering on B16-F10 cells in vivo. (**A** and **B**) Effect on metastasis in C57BL/6 mice injected in the tail vein with 10^6 B7h^{high} B16-F10 cells and treated daily with either the mouse ICOS-Fc ($n = 3$), human ^{F119S}ICOS-Fc ($n = 3$), or the same volume of PBS (control group, $n = 3$). The lung metastases were analyzed either after 3 d (on tissue sections stained with H&E) (A) or after 2 wk by counting the detectable tumor nodules on the lung surface (B); (**C**) infiltrating cells from the 3-d experiment were harvested and used for the real-time PCR analysis of IL-17A, IL-10, RORc, and Foxp3 expression; the data are normalized for the expression in the control mice (control expression set at 100%). (**D**) Effect on β-Pix expression in s.c. tumors treated with an intratumoral injection of either the mouse ICOS-Fc, human ^{F119S}ICOS-Fc, or the same volume of PBS. The C57BL/6 mice were s.c. injected with 10^6 B7h^{high} B16-F10 cells, and the tumors were treated when they reached 4 mm in diameter. The β-Pix expression was evaluated via Western blot in the lysates of the tumor tissue. The data are expressed as the mean ± SEM and were obtained from three experiments ($*p < 0.05$, $**p < 0.01$).

reports indicate that EMT is also involved in the emergence of cancer stem cells and contributes to drug resistance (24). A classical inducer of EMT is HGF (also known as scatter factor), which promotes an "invasive growth" of epithelial cells that is characterized by the disruption of intercellular contacts and the induction of cell motility, survival, and proliferation (19, 25). Our experiments on HepG2 cells show that ICOS-Fc effectively impairs their HGF-induced scattering by preserving the epithelial morphology and strongly reducing the HGF-induced migration. These findings suggest that ICOS-Fc could also affect EMT in vivo and decrease the metastatic potential of tumor cells.

To successfully metastasize (after the downregulation of cell-to-cell junctions and the acquisition of a migratory phenotype), tumor cells must invade the extracellular matrix and intravasate; they will then disseminate and become sites of origin for future metastases. Cell movement across the tissues plays a crucial role in several of these steps. Thus, a major aim in modern cancer therapy strategies is to counteract metastatic spreading by targeting the factors involved in the migratory activity of tumor cells. This has been mainly achieved using antagonists of the molecules involved in the adhesion of these cells to the extracellular matrix (26), as well as antagonists of proteases that facilitate cell migration by degrading the extracellular matrix (27–29). Unfortunately, none of these compounds has yet reached the market, primarily because of poor in vivo antitumor activity, unsuitable therapeutic index, or the rapid development of chemoresistance. This work suggests that B7h may be a novel target for these therapies because ICOS-Fc inhibits the migration of several tumor cell lines in vitro. This effect is not ascribable to drug toxicity because the proliferation and survival of tumor cells are not affected by ICOS-Fc. Moreover, this effect is specific; it is not detected in tumor cell lines expressing low levels of B7h.

This underlines a potential pharmacological limitation of ICOS-Fc, the efficacy of which is expected to be restricted to B7h^{high} tumors. It is intriguing that the migratory response to FCS appeared to be weaker in the B7h^{low} than in the B7h^{high} cell lines and that the B7h^{low} B16-F10 cells displayed lower migratory activity than their B7h^{high} counterparts, which suggests that B7h may play a direct role in cell migration. The antimetastatic effect of ICOS-Fc is supported by our in vivo experiments showing that treatment with ICOS-Fc inhibits the migration of both a human (CF-PAC1 Luc) and a mouse (B16-F10) tumor cell line into the lungs in mice. It is noteworthy that this effect was induced by both the human and the mouse ICOS-Fc in the CF-PAC1 Luc human/mouse model, which indicates that the effect was ascribable to the triggering of both varieties of B7h on the tumor cells, as well as the ECs. The human ICOS-Fc does not bind the mouse B7h, and the mouse ICOS-Fc weakly binds the human B7h (data not shown).

These data strengthen those obtained from previous research showing that ICOS-Fc inhibits tumor cell adhesion to ECs by acting on both the tumor cells and the ECs (11). Moreover, in the B16-F10 model, treatment with ICOS-Fc increased the expression of IL-17A and RORc, and decreased the expression of IL-10 and Foxp3; this suggests that ICOS-Fc may also exert positive effects on the antitumor immune response by increasing the Th17/Treg ratio. This observation is in accordance with reports showing that the triggering of B7h in immature mouse DCs induces partial maturation with the prominent augmentation of IL-6 secretion (17), as

well as reports indicating that IL-6 supports the conversion of $Foxp3^+CD4^+$ Tregs to Th17 cells (30). Moreover, we found that B7h triggering in human DCs increases the secretion of IL-23 (which is involved in Th17 expansion and survival) and supports Th17 cell activity (18). Finally, ICOS triggering in T cells (which is blocked by ICOS-Fc) is involved in the differentiation of both Tregs and Th17 cells (17, 31–33); however, its support of Treg differentiation prevails in the tumor environment (34, 35).

The possibility that ICOS-Fc may also affect tumor angiogenesis is suggested by the finding that it substantially inhibits the migration of vascular ECs. However, it does not inhibit EC proliferation or angiogenesis, as determined via the tubulogenesis and the sprouting assays, which indicates that the residual migratory potential of ECs is sufficient for these in vitro assays. However, this does not rule out the possibility that ICOS-Fc may be effective in limiting conditions in vivo. The antiangiogenic potential of ICOS-Fc is intriguing because the survival of the primary tumor beyond a certain size requires neovascularization of the tumor mass, and tumor-associated vessels represent a preferential pathway for metastasization to distant sites. Thus, controlling tumor-associated angiogenesis may limit cancer progression (21). However, clinical results from studies using individual antivascular agents have been unsatisfactory and have required the combinatorial use of conventional anticancer drugs and antivascular agents (22). Therefore, novel antivascular agents targeting B7h would be welcome in antitumor therapy.

In previous works, we demonstrated that B7h triggering inhibits the activation of the ERK and p38 axis induced in ECs via various proadhesive stimuli. This leads to cytoskeleton modifications with the disruption of the VE-cadherin/β-catenin complex and the formation of stress fibers involved in increasing the endothelial permeability and enabling the transendothelial migration of cancer cells (11). However, this is not a general effect because it was not detected in tumor cell lines (11) or DCs (18). In contrast, in DCs (18), ECs, and tumor cells (Fig. 6), ICOS-Fc downregulates the expression of β-Pix, which is a Rac-1 activator that is recruited by activated integrins and is required for rapid nascent adhesion turnover. Intriguingly, the downregulation of β-Pix expression is known to prevent cell spreading and lamellipodial formation, and to increase Rac1 activity (36, 37). Moreover, in ECs and tumor cells, B7h triggering inhibits the phosphorylation of FAK, which is a key mediator of signaling through integrins. The overexpression and activation of FAK have been found in a variety of human cancers and have been involved in cancer migration, invasion, EMT, and angiogenesis (38). FAK signaling has also been shown to promote angiogenesis in both embryonic development and tumor angiogenesis, and the increased phosphorylation and activation of FAK have been correlated with increased EC migration into wounded monolayers (39). The signaling pathways activated by B7h are presently unknown. In DCs, the engagement of B7.1 or B7.2 with CTLA4-Ig leads to the STAT-1–mediated production of IDO and decreased tryptophan levels (40, 41); however, it is unclear whether a similar signaling pathway is also activated by B7h.

Upon extrapolating these data to physiological conditions, it may be suggested that the physiological role of B7h-mediated signaling is based on its effect on invasion, which is involved not only in tumor progression (42), but also in tissue remodeling during embryonic development, wound healing, angiogenesis, and immune responses. In accordance with this possibility, the repair of excisional wounds was dramatically delayed in mice deficient in either ICOS or B7h; these mice showed decreased keratinocyte migration, angiogenesis, granulation tissue formation, and diminished infiltration of T cells, macrophages, and neutrophils (43). One possibility is that $B7h^+$ cells, which are recruited from the blood and the surrounding tissues for tissue defense and repair, are arrested in the injured tissue via B7h interacting with the ICOS that is expressed by the infiltrating T cells. Therefore, a defective B7h–ICOS interaction may eventually affect the accumulation of infiltrating cells in the injured tissue.

In conclusion, our data indicate that ICOS-Fc may be an effective antimetastasis drug acting on ECs and tumor cells both in vitro and in vivo. Therefore, ICOS-Fc (which affects cancer cell migration without severe toxic effects) may be a sound tool in cancer therapy that acts on several aspects of tumor progression.

Acknowledgments

We are grateful to the Obstetrics and Gynecology Unit, Martini Hospital, Torino, for providing human umbilical cords.

Disclosures

The authors have no financial conflicts of interest.

References

1. Greenwald, R. J., G. J. Freeman, and A. H. Sharpe. 2005. The B7 family revisited. *Annu. Rev. Immunol.* 23: 515–548.
2. Okazaki, T., Y. Iwai, and T. Honjo. 2002. New regulatory co-receptors: inducible co-stimulator and PD-1. *Curr. Opin. Immunol.* 14: 779–782.
3. Hutloff, A., A. M. Dittrich, K. C. Beier, B. Eljaschewitsch, R. Kraft, I. Anagnostopoulos, and R. A. Kroczek. 1999. ICOS is an inducible T-cell co-stimulator structurally and functionally related to CD28. *Nature* 397: 263–266.
4. Buonfiglio, D., M. Bragardo, S. Bonissoni, V. Redoglia, R. Cauda, S. Zupo, V. L. Burgio, H. Wolff, K. Franssila, G. Gaidano, et al. 1999. Characterization of a novel human surface molecule selectively expressed by mature thymocytes, activated T cells and subsets of T cell lymphomas. *Eur. J. Immunol.* 29: 2863–2874.
5. Buonfiglio, D., M. Bragardo, V. Redoglia, R. Vaschetto, F. Bottarel, S. Bonissoni, T. Bensi, C. Mezzatesta, C. A. Janeway, Jr., and U. Dianzani. 2000. The T cell activation molecule H4 and the CD28-like molecule ICOS are identical. *Eur. J. Immunol.* 30: 3463–3467.
6. Redoglia, V., U. Dianzani, J. M. Rojo, P. Portolés, M. Bragardo, H. Wolff, D. Buonfiglio, S. Bonissoni, and C. A. Janeway, Jr. 1996. Characterization of H4: a mouse T lymphocyte activation molecule functionally associated with the CD3/T cell receptor. *Eur. J. Immunol.* 26: 2781–2789.
7. Swallow, M. M., J. J. Wallin, and W. C. Sha. 1999. B7h, a novel costimulatory homolog of B7.1 and B7.2, is induced by TNFalpha. *Immunity* 11: 423–432.
8. Yoshinaga, S. K., J. S. Whoriskey, S. D. Khare, U. Sarmiento, J. Guo, T. Horan, G. Shih, M. Zhang, M. A. Coccia, T. Kohno, et al. 1999. T-cell co-stimulation through B7RP-1 and ICOS. *Nature* 402: 827–832.
9. Wang, S., G. Zhu, A. I. Chapoval, H. Dong, K. Tamada, J. Ni, and L. Chen. 2000. Costimulation of T cells by B7-H2, a B7-like molecule that binds ICOS. *Blood* 96: 2808–2813.
10. Xiao, J. X., P. S. Bai, B. C. Lai, L. Li, J. Zhu, and Y. L. Wang. 2005. B7 molecule mRNA expression in colorectal carcinoma. *World J. Gastroenterol.* 11: 5655–5658.
11. Dianzani, C., R. Minelli, R. Mesturini, A. Chiocchetti, G. Barrera, S. Boscolo, C. Sarasso, C. L. Gigliotti, D. Sblattero, J. Yagi, et al. 2010. B7h triggering inhibits umbilical vascular endothelial cell adhesiveness to tumor cell lines and polymorphonuclear cells. *J. Immunol.* 185: 3970–3979.
12. Minelli, R., L. Serpe, P. Pettazzoni, V. Minero, G. Barrera, C. L. Gigliotti, R. Mesturini, A. C. Rosa, P. Gasco, N. Vivenza, et al. 2012. Cholesteryl butyrate solid lipid nanoparticles inhibit the adhesion and migration of colon cancer cells. *Br. J. Pharmacol.* 166: 587–601.
13. Mesturini, R., S. Nicola, A. Chiocchetti, I. S. Bernardone, L. Castelli, T. Bensi, M. Ferretti, C. Comi, C. Dong, J. M. Rojo, et al. 2006. ICOS cooperates with CD28, IL-2, and IFN-gamma and modulates activation of human naïve CD4+ T cells. *Eur. J. Immunol.* 36: 2601–2612.
14. Mesturini, R., C. L. Gigliotti, E. Orilieri, G. Cappellano, M. F. Soluri, E. Boggio, A. Woldetsadik, C. Dianzani, D. Sblattero, A. Chiocchetti, et al. 2013. Differential induction of IL-17, IL-10, and IL-9 in human T helper cells by B7h and B7.1. *Cytokine* 64: 322–330.
15. Franko, J. L., and A. D. Levine. 2009. Antigen-independent adhesion and cell spreading by inducible costimulator engagement inhibits T cell migration in a PI-3K-dependent manner. *J. Leukoc. Biol.* 85: 526–538.
16. Yong, P. F., U. Salzer, and B. Grimbacher. 2009. The role of costimulation in antibody deficiencies: ICOS and common variable immunodeficiency. *Immunol. Rev.* 229: 101–113.
17. Tang, G., Q. Qin, P. Zhang, G. Wang, M. Liu, Q. Ding, Y. Qin, and Q. Shen. 2009. Reverse signaling using an inducible costimulator to enhance immunogenic function of dendritic cells. *Cell. Mol. Life Sci.* 66: 3067–3080.
18. Occhipinti, S., C. Dianzani, A. Chiocchetti, E. Boggio, N. Clemente, C. L. Gigliotti, M. F. Soluri, R. Minelli, R. Fantozzi, J. Yagi, et al. 2013. Triggering of B7h by the inducible costimulator modulates maturation and migration of monocyte-derived dendritic cells. *J. Immunol.* 190: 1125–1134.
19. Pan, F. Y., S. Z. Zhang, N. Xu, F. L. Meng, H. X. Zhang, B. Xue, X. Han, and C. J. Li. 2010. Beta-catenin signaling involves HGF-enhanced HepG2 scattering through activating MMP-7 transcription. *Histochem. Cell Biol.* 134: 285–295.

20. Hanahan, D., and R. A. Weinberg. 2011. Hallmarks of cancer: the next generation. *Cell* 144: 646–674.
21. Weis, S. M., and D. A. Cheresh. 2011. Tumor angiogenesis: molecular pathways and therapeutic targets. *Nat. Med.* 17: 1359–1370.
22. Mizukami, Y., J. Sasajima, T. Ashida, and Y. Kohgo. 2012. Abnormal tumor vasculatures and bone marrow-derived pro-angiogenic cells in cancer. *Int. J. Hematol.* 95: 125–130.
23. Hayot, C., O. Debeir, P. Van Ham, M. Van Damme, R. Kiss, and C. Decaestecker. 2006. Characterization of the activities of actin-affecting drugs on tumor cell migration. *Toxicol. Appl. Pharmacol.* 211: 30–40.
24. Singh, A., and J. Settleman. 2010. EMT, cancer stem cells and drug resistance: an emerging axis of evil in the war on cancer. *Oncogene* 29: 4741–4751.
25. Boccaccio, C., and P. M. Comoglio. 2006. Invasive growth: a MET-driven genetic programme for cancer and stem cells. *Nat. Rev. Cancer* 6: 637–645.
26. Sawyer, T. K. 2004. Cancer metastasis therapeutic targets and drug discovery: emerging small-molecule protein kinase inhibitors. *Expert Opin. Investig. Drugs* 13: 1–19.
27. Zucker, S., J. Cao, and W. T. Chen. 2000. Critical appraisal of the use of matrix metalloproteinase inhibitors in cancer treatment. *Oncogene* 19: 6642–6650.
28. Coussens, L. M., B. Fingleton, and L. M. Matrisian. 2002. Matrix metalloproteinase inhibitors and cancer: trials and tribulations. *Science* 295: 2387–2392.
29. Overall, C. M., and C. López-Otín. 2002. Strategies for MMP inhibition in cancer: innovations for the post-trial era. *Nat. Rev. Cancer* 2: 657–672.
30. Komatsu, N., K. Okamoto, S. Sawa, T. Nakashima, M. Oh-hora, T. Kodama, S. Tanaka, J. A. Bluestone, and H. Takayanagi. 2014. Pathogenic conversion of Foxp3+ T cells into TH17 cells in autoimmune arthritis. *Nat. Med.* 20: 62–68.
31. Park, H., Z. Li, X. O. Yang, S. H. Chang, R. Nurieva, Y. H. Wang, Y. Wang, L. Hood, Z. Zhu, Q. Tian, and C. Dong. 2005. A distinct lineage of CD4 T cells regulates tissue inflammation by producing interleukin 17. *Nat. Immunol.* 6: 1133–1141.
32. Paulos, C. M., C. Carpenito, G. Plesa, M. M. Suhoski, A. Varela-Rohena, T. N. Golovina, R. G. Carroll, J. L. Riley, and C. H. June. 2010. The inducible costimulator (ICOS) is critical for the development of human T(H)17 cells. *Sci. Transl. Med.* 2: 55ra78.
33. Ito, T., S. Hanabuchi, Y. H. Wang, W. R. Park, K. Arima, L. Bover, F. X. Qin, M. Gilliet, and Y. J. Liu. 2008. Two functional subsets of FOXP3+ regulatory T cells in human thymus and periphery. *Immunity* 28: 870–880.
34. Strauss, L., C. Bergmann, M. J. Szczepanski, S. Lang, J. M. Kirkwood, and T. L. Whiteside. 2008. Expression of ICOS on human melanoma-infiltrating CD4+CD25highFoxp3+ T regulatory cells: implications and impact on tumor-mediated immune suppression. *J. Immunol.* 180: 2967–2980.
35. Martin-Orozco, N., Y. Li, Y. Wang, S. Liu, P. Hwu, Y. J. Liu, C. Dong, and L. Radvanyi. 2010. Melanoma cells express ICOS ligand to promote the activation and expansion of T-regulatory cells. *Cancer Res.* 70: 9581–9590.
36. Schmidt, M. H., K. Husnjak, I. Szymkiewicz, K. Haglund, and I. Dikic. 2006. Cbl escapes Cdc42-mediated inhibition by downregulation of the adaptor molecule betaPix. *Oncogene* 25: 3071–3078.
37. Lee, J., I. D. Jung, W. K. Chang, C. G. Park, D. Y. Cho, E. Y. Shin, D. W. Seo, Y. K. Kim, H. W. Lee, J. W. Han, and H. Y. Lee. 2005. p85 beta-PIX is required for cell motility through phosphorylations of focal adhesion kinase and p38 MAP kinase. *Exp. Cell Res.* 307: 315–328.
38. Zhao, J., and J. L. Guan. 2009. Signal transduction by focal adhesion kinase in cancer. *Cancer Metastasis Rev.* 28: 35–49.
39. Romer, L. H., N. McLean, C. E. Turner, and K. Burridge. 1994. Tyrosine kinase activity, cytoskeletal organization, and motility in human vascular endothelial cells. *Mol. Biol. Cell* 5: 349–361.
40. Orabona, C., U. Grohmann, M. L. Belladonna, F. Fallarino, C. Vacca, R. Bianchi, S. Bozza, C. Volpi, B. L. Salomon, M. C. Fioretti, et al. 2004. CD28 induces immunostimulatory signals in dendritic cells via CD80 and CD86. *Nat. Immunol.* 5: 1134–1142.
41. Grohmann, U., C. Orabona, F. Fallarino, C. Vacca, F. Calcinaro, A. Falorni, P. Candeloro, M. L. Belladonna, R. Bianchi, M. C. Fioretti, and P. Puccetti. 2002. CTLA-4-Ig regulates tryptophan catabolism in vivo. *Nat. Immunol.* 3: 1097–1101.
42. Sliva, D. 2004. Signaling pathways responsible for cancer cell invasion as targets for cancer therapy. *Curr. Cancer Drug Targets* 4: 327–336.
43. Maeda, S., M. Fujimoto, T. Matsushita, Y. Hamaguchi, K. Takehara, and M. Hasegawa. 2011. Inducible costimulator (ICOS) and ICOS ligand signaling has pivotal roles in skin wound healing via cytokine production. *Am. J. Pathol.* 179: 2360–2369.

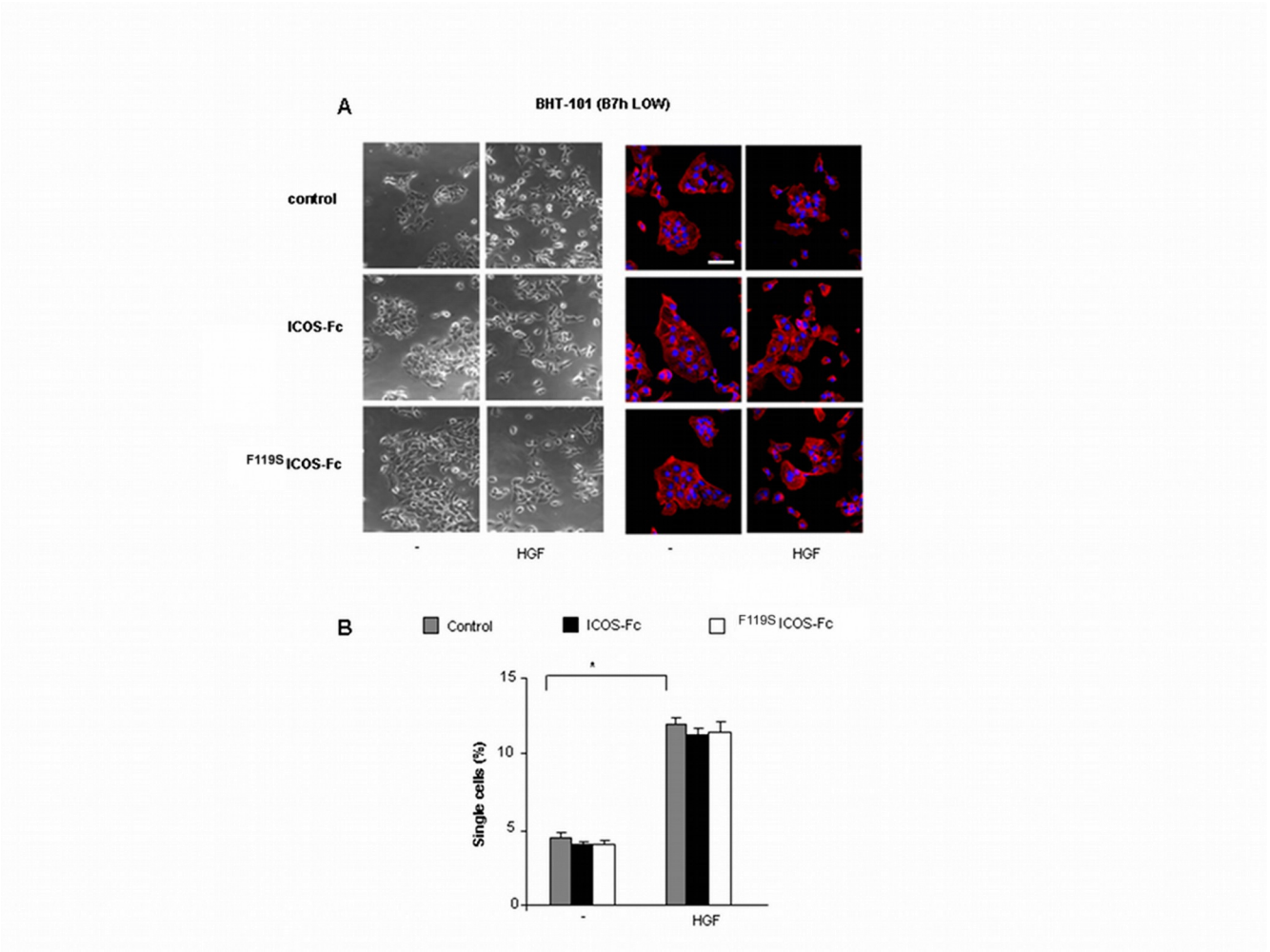

FIGURE S1: ICOS-Fc does not affect HGF induced cells scatter in BHT-101.Cells were treated for 24 h with or without HGF (50 ng/ml), ICOS-Fc (2 µg/ml) or ^{F119S}ICOS-Fc (2 µg/ml). (**A**) Cells were photographed by phase contrast (*left panel*) or stained with Phalloidin-Alexa-Fluor 546 (red) / TO-PRO 3 (blue) (*right panel*) and imaged by confocal microscopy. Scale bar 40 µm. (**B**) Percentage of disaggregated single cells (mean±SEM of 4 experiments); at least 100 cells were counted for each point (* $P < 0.01$).

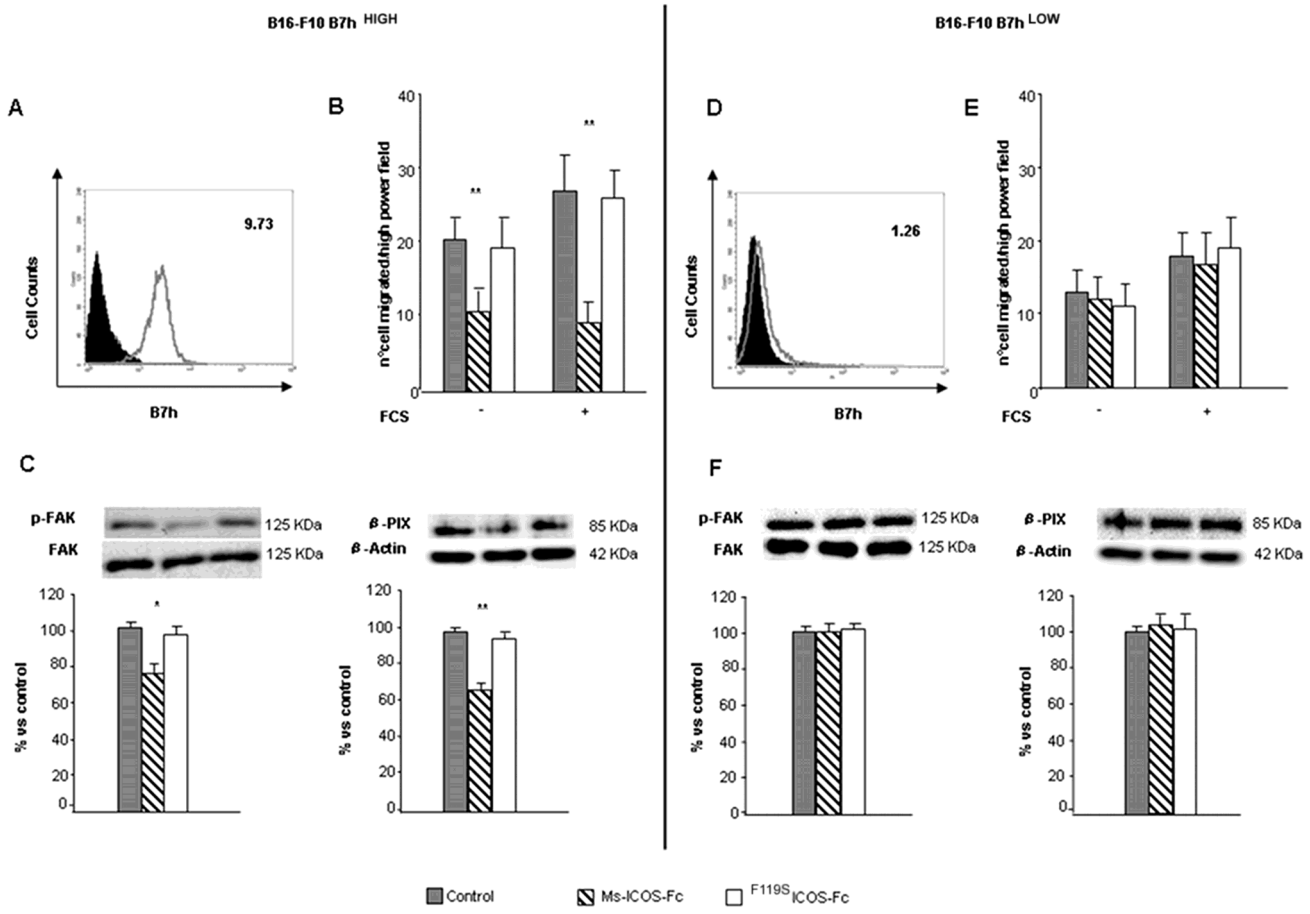

FIGURE S2: Effect of ICOS-Fc on B7h^{high} and B7h^{low} B16-F10 cells *in vitro*. (**A, D**) Cytofluorimetric analysis of B7h expression performed as in Fig. 1. (**B, E**) Effect of ICOS-Fc on cell migration in the Boyden chamber assay performed as in Fig. 2. (**C, F**) Effect of ICOS-Fc on FAK phosphorylation (*left panel*) and β-Pix expression (*right panel*) performed as in Fig. 5. Data are expressed as mean±SEM from 3 independent experiments (** P<0.01, * P<0.05 versus the control).